

# Systematic Microwave Source Motions along Flare-arcade Observed by Nobeyama Radioheliograph and AIA/SDO

Sujin KIM

*Nobeyama Solar Radio Observatory / NAOJ, Nagano, 384-1305, Japan*

*sujin.kim@nao.ac.jp*

Satoshi MASUDA

*STElab / Nagoya University, Nagoya, 464-8601 Japan*

*masuda@stelab.nagoya-u.ac.jp*

Kiyoto SHIBASAKI

*Nobeyama Solar Radio Observatory / NAOJ, Nagano, 384-1305, Japan*

*shibasaki.kiyoto@nao.ac.jp*

and

Su-Chan BONG

*Korea Astronomy and Space Science Institute, Daejeon, 305-348, Republic of Korea*

*scbong@kasi.re.kr*

(Received ; accepted )

## Abstract

We found systematic microwave source motions along a flare-arcade using Nobeyama Radioheliograph (NoRH) 17 GHz images. The motions were associated with a X-class disk flare which occurred on 15th February 2011. For this study, we also used EUV images from Atmospheric Imaging Assembly (AIA) and magnetograms from Helioseismic and Magnetic Imager (HMI) onboard Solar Dynamics Observatory, and multi-channel microwave data from Nobeyama Radiopolarimeters (NoRP) and Korean Solar Radio Burst Locator (KSRBL). We traced centroids of the microwave source observed by NoRH 17 GHz during the flare and found two episodes of the motion with several facts: 1) The microwave source moved systematically along the flare-arcade, which was observed by the AIA 94 Å in a direction parallel to the neutral line. 2) The period of each episode was 5 min and 14 min, respectively. 3) Estimated parallel speed was 34 km s<sup>-1</sup> for the first episode and 22 km s<sup>-1</sup> for the second episode. The spectral slope of microwave flux above 10 GHz obtained by NoRP and KSRBL was negative for both episodes, and for the last phase of the second episodes, it was flat with the flux of 150 sfu. The negative spectrum and the flat with high flux

indicate that the gyrosynchrotron emission from accelerated electrons was dominant during the source motions. The sequential images from the AIA 304 Å and 94 Å channels revealed that there were successive plasma eruptions and each eruption was initiated just before the start time of the microwave sources motion. Based on the results, we suggest that the microwave source motion manifests the displacement of the particle acceleration site caused by plasma eruptions.

**Key words:** Sun:flares, Sun:corona, Sun:radio radiation, Sun:particle emission

## 1. Introduction

Emissions generated by high energy particles during solar flares provide key information of accelerations, injections, and trap-precipitations in the flaring structures. In practice, during flares, the microwave in high frequency regime can capture optically thin gyrosynchrotron emission from accelerated electrons. Nobeyama Radioheliograph (Nakajima et al. 1994) has been taking images of the full sun, including flares as well as the quiet sun, at 17 GHz since 1992 and at 34 GHz since 1994. Using these microwave data, many authors have studied the distribution of accelerated electrons and its dynamics in flaring loops (Kundu et al. 2001; Melnikov et al. 2002; Yokoyama et al. 2002; Huang & Nakajima 2009; Reznikova et al. 2010; Asai et al. 2013). Simultaneously, particle kinematics in flare loops have been established by models and simulations based on NoRH observations (Melnikov et al. 2002; Melnikov et al. 2005; Minoshima et al. 2008; Minoshima et al. 2010).

When flares occur, accelerated high energy electrons are generally revealed in microwaves by gyrosynchrotron emission in the magnetic loops and in hard X-ray (HXR) by bremsstrahlung at the footpoints of the loops (Shibata et al. 1995). Thus, a position of a source observed in the HXR and microwaves can manifest a macroscopic view of flare dynamics as a direct indicator of the change of the magnetic field configuration of flaring region. And a motion of the source position can be regarded as a displacement of a site where the injection and the acceleration take place. The HXR bremsstrahlung from energetic electrons at the footpoints of the magnetic loop has shown various patterns of source motions (Krucker et al. 2003; Bogachev & Somov 2005; Grigis & Benz 2005; Liu et al. 2009; Liu et al. 2011). Bogachev & Somov (2005) studied the motions of two footpoints linked to opposite sides of the magnetic neutral line (NL) during 31 flares and categorized the major patterns of the motions into three types: perpendicular, anti-parallel, and parallel to the NL. They interpreted the former two types as a standard reconnection model with simple or sheared overlying magnetic field and the last type was speculated as a chromospheric signature of a displacement of the particle acceleration region in the corona. **Similarly to HXR footpoints motion, Reznikova et al. (2010) found that one footpoint of microwave flare loop moved while the other was stationary. The**

authors interpreted it as an unshearing motion of the magnetic loops resulting from the energy releasing process during the flare. Recently, Fleishman et al. (2013) reported the displacement of the centroid of microwave source during the flare. It appeared in the edge of the HXR source, which was located near the top of the thermal loop, during the impulsive phase, and then moved to the center of the HXR source during the decay phase. They speculated that the microwave emission dominated the acceleration site of electrons during the early phase of the flare and then dominated the trapping site of accelerated electrons. This centroid position and motion of microwave source can give a clue to solve dynamics of high energy particles during the flare through showing direct position where the particles are accelerated and trapped.

In this paper, for the first time, we present systematic motions of the microwave source centroid along the flare-arcade system. The motion recurred once again in the similar way with the first episode during the flare. It was investigated using available high time cadence multi-wavelength data: microwave imaging data from NoRH 17 GHz, and EUV imaging data from 304 and 94 Å channels of Atmospheric Imaging Assembly (AIA: Lemen et al. 2012) and magnetograms of Helioseismic and Magnetic Imager (HMI: Scherrer et al. 2012) onboard Solar Dynamics Observatory. Also, we have examined HXR sources observed by RHESSI, but they showed no systematic motion. Thus, we focused on the microwave source motion in the observations. The discrepancy between the motions in HXR and microwaves is discussed in §3. In §2, we describe the morphological evolution in EUV, the source motions in microwave, and the microwave spectra during two episodes of the motions. In §3, we discuss possible cause of the microwave source motions during the flare.

## 2. Observations

We have examined a X2.2 flare which occurred on 15 February 2011. The flare took place in Active Region 11158 which was located near the disk center, S20W11. Figure 1 shows the light curves of fluxes of GOES X-rays (top), NoRP 17 and 35 GHz (middle), and RHESSI 25-100 keV (bottom). The microwave flare started at 01:48:19 UT and peaked at 01:55:20 UT. There was another peak before main peak at 01:53:30 UT. These two peaks are separated by the period of a sudden flux drop. The flux curve of HXR in the bottom panel of Figure 1 also exhibits consistent time profile with the microwave flux, which has a drastic drop between two peaks. It suggests that there were two distinct energy release processes resulting in two peaks in the time profile of the flux. In this section, we present plasma eruptions and microwave source motions in which overall observations are intimately related with each other in timing aspect as appears in the flux curves. And we have examined the microwave spectra and flux value to know the emission mechanism of moving sources.

## 2.1. Plasma Eruptions

EUV multi-channels of AIA **aim for** investigation of multi-thermal plasma in the solar atmosphere from the chromosphere to the corona. In order to look at the emission from the chromosphere and the corona simultaneously, we have examined two EUV channels. One is 304 Å channel, which contains a contribution from He II formed at 0.05 MK, and the other is 94 Å channel, which contains lines from Fe XVIII, formed at 7 MK (Lemen et al. 2012). The AIA data were taken with a spatial resolution of 1.2 " every 12 seconds. Figure 2 shows sequential images of two channels from top to bottom during the flare. The 304 Å channel exhibits the formation and the development of the two-ribbon at the chromospheric footpoints. The neutral line (a black line in Figure 2d) is located on the center of the two-ribbon. The neutral line, where the positive polarity and the negative polarity are encountered, was determined by magnetogram obtained from HMI (see a yellow line in Figure 4). At the same time, the 94 Å channel shows the formation of flare-arcade loops filled with hot plasma during the flaring process. The sequential images of both channels reveal that there were two successive eruptions during impulsive phase of the flare. First eruption (1st ER) is shown indirectly in 94 Å images as a rapid radial expansion of ambient coronal loops. Figure 2e and 2f show one of them which expands along white arrows. The ambient coronal loops began to expand just before the flare start time, and finally, they shrunk and/or disappeared. Second eruption (2nd ER) appeared in the 304 Å channel as a bulk plasma eruption. It was initiated in the north-east site of the two-ribbon system around 01:53 UT and erupted along the direction of a white arrow in Figure 2c. Coronal mass ejections (CME) observed by Large Angle Spectroscopic Coronagraph (LASCO: Brueckner et al. 1995) onboard Solar and Heliospheric Observatory (SOHO: Domingo et al. 1995) have been reported in on-line CME catalog<sup>1</sup>. According to the catalog, the eruption related to our flare was developed into a halo CME. Considering the radial expansion and timing of the first eruption, it is plausible that it results in the observed halo CME. On the other hands, it seems that the second eruption could not be seen in the LASCO images by screening of huge and strong emission of the first CME and/or by a failure of escape from the solar atmosphere.

## 2.2. Microwave Source Motions

We have investigated the source motions using NoRH 17 GHz images with 1 second time cadence. Synthesized images of 17 GHz have a spatial resolution of 10 ". We determined the source centroid as a center of 95 % level of maximum brightness temperature ( $T_B$ ). As the result, we found smooth trajectory of the source motions. Figure 3 shows two episodes of the microwave source motion with contours of  $T_B$  at 17 GHz on the AIA 94 Å image. For the first episode (here after EP1) in the left panel of Figure 3, a compact microwave source appears on the east site of the flaring region at 01:48:19 UT and then migrates toward the north-west

---

<sup>1</sup> [http://cdaw.gsfc.nasa.gov/CME\\_list](http://cdaw.gsfc.nasa.gov/CME_list)

direction along the flare arcade until 01:53:34 UT. The period of the motion is around 5 minutes. The second episode (here after EP2) in the right panel of figure 3 begins near the start position of EP1 at 01:55:30 UT and the source moves toward the north-west direction along the flare arcade until 02:10:00 UT. The period of the motion is around 14 minutes. The source centroids during each episode are shown in the bottom panels of Figure 3, with colors coded by time. The uniformly distributed color manifests that the sequential motion progressed systematically. Note that the source positions are located near or on the top of the flare-arcade seen in the 94 Å image. If the maximum of microwave emission are due to gyrosynchrotron emission of accelerated electrons during two episodes, then the results imply that the accelerated particles are generated at the loop-top or high in the corona and injected into the loop-top. Thus, one can speculate that the displacement of the acceleration site comes into view as a microwave source motion during the flare. In order to investigate the source motion in detail, we plot all of the source centroid on the magnetogram obtained by HMI (Figure 4). Source positions are elongated parallel to the neutral line which is denoted by a yellow line in Figure 4. Figure 5 shows the variation of the source position with time in the direction parallel to the NL (top) and perpendicular to the NL (bottom). The parallel motion shows consistent propagation along the NL and its speeds estimated by the linear fit was  $37 \text{ km s}^{-1}$  for EP1 and  $22 \text{ km s}^{-1}$  for EP2. Meantime, the perpendicular motion is converging toward the NL with a speed of  $-9 \text{ km s}^{-1}$  for EP1 and  $-3 \text{ km s}^{-1}$  for EP2. Considering the center of the microwave sources are located near the loop-top region (bottom panels of Figure 3), the converging motion toward the NL may reflect that the loop-top position of flare loops moves toward the NL.

### 2.3. Microwave Spectra

Nobeyama Radiopolarimeters (NoRP: Nakajima et al. 1985) has multi-channels of 1, 2, 3.75, 9.4, 17, 35, and 80 GHz. It detects total flux from the sun with a time cadence of 0.1 s. During flares, microwave spectra obtained by NoRP can be used to identify the emission mechanism in high frequency regime, gyrosynchrotron emission from mildly relativistic electrons or free-free emission due to thermal electrons (see Dulk 1985). In this study, low frequency channels of 1 and 2 GHz were not used because they didn't follow gyrosynchrotron nor thermal free-free emission. 80 GHz also wasn't used due to no detection. In addition to the NoRP data, we have examined continuous spectra using Korean Solar Radio Burst Locator (KSRBL: Dou et al. 2009) which is a radio spectrometer covering 0.245, 0.410, and 0.5—18 GHz band with 1 second time cadence and 1 MHz frequency resolution. **Due to the characteristics of the spiral feed in use, it observes only the right-hand circular polarization (RCP) and the observed spectra are modulated in a regular pattern depending on the source location. As microwave spectra are expected to follow a power law (Dulk 1985), the modulation pattern can be removed by minimizing the average deviation from a smooth fit of the demodulated spectra, and it results in the ability to**

locate the source position within  $2'$ . To compare with the NoRP data, we matched the flux of the KSRBL at quiet time to the Stokes I flux of US Air Force Radio Solar Telescope Network (RSTN: Guidice et al. 1981) assuming no polarization. Since strong interferences appeared below 9.5 GHz, we only used the frequency band above this frequency.

Figure 6 shows microwave spectra obtained by NoRP four channels, 3.75, 9.4, 17, and 35 GHz. Each spectrum, from the top to bottom, was obtained near the start time and the end time of each episode. During EP1 (Figure 6a and 6b), microwave spectra demonstrate that the gyrosynchrotron emission is consistently dominant: decreasing flux with frequency in high frequency regime with a turnover frequency around 9.4 GHz (vertical dashed line in Figure 6). The KSRBL continuous spectra is in alignment with the straight line connecting fluxes at 9.4 GHz to 17 GHz of the NoRP. It confirms that the turnover frequency is not higher than 10 GHz. On the other hands, during EP2, the gyrosynchrotron emission is dominant only during initial phase (Figure 6c) and then the spectra become flat with constant flux of  $\sim 150$  sfu in high frequency regime (Figure 6d). One should note that 150 sfu is too high value just to be generated by thermal free-free process, but rather there would be significant contribution from gyrosynchrotron emission. White et al. (2011) have presented that GOES X1 flare produces an order of 10–50 sfu of thermal emission from optically thin flare plasma above 10 GHz. We estimated expected radio thermal emission based on the radiative transfer equation for thermal free-free emission of optically thin plasma (Dulk 1985) using physical quantities of plasma temperature, 15 MK, and emission measure,  $1 \times 10^{49} \text{ cm}^{-3}$ , which were derived from GOES two-channels (see White et al. 2005). As the result, we found that the contribution of microwave thermal emission was around 90 sfu which is much less than the observed flux. Considering the compact source for EP1 and broad source covering flare arcade for EP2, thermal emission were enhanced during initial phase of nonthermal flaring process so that it might come into view as the broad source covering large area of flaring region during EP2.

### 3. Summary and Discussion

We have investigated microwave source motions during X-class flare which occurred on 15 February 2011 using NoRH 17 GHz, AIA two channels of 304 and 94 Å, and HMI magnetogram. As the results, we found two episodes of microwave source motion along the flare-arcade and the neutral line. All of the source positions were located near the top of the flare loops constituting the flare-arcade. Interestingly, two episodes of source motion started just after the initiation of two successive plasma eruptions revealed by sequential images of the 304 and the 94 Å. It suggests that the plasma eruptions may trigger the microwave source motion and may govern the systematic motion along the flare-arcade and the NL.

The standard model of the flare (e.g. Hirayama 1974; Shibata et al. 1995; Forbes & Acton 1996) describes the energy release process with several key sequential activities: 1) Rising flux



rope system, 2) bi-directional magnetic field lines closing by inward pressure in between them where the flux rope sweeps through, 3) reconnection and then release of accelerated particles toward the rising flux rope and the flare loops. When the accelerated particles are injected and trapped into newly formed magnetic loops by reconnection, gyrosynchrotron emission from them is readily generated in microwave and its position would be on or near the loop-top region. We found that the eruptions, which are a manifestation of rising flux ropes, appeared in the 304 and 94 Å images (Figure 2) and halo CME was followed in SOHO/LASCO. Hence, in the picture of the standard model, the source position on the loop-top implies that the accelerated electrons were injected into the loop-top directly from high corona (Melnikov et al. 2002) or the fast contraction of newly formed loop by reconnection accelerated electrons in the loop-top up to relativistic energies (Somov & Kosugi 1997; Bogachev & Somov 2005). In fact, the loop-top concentration of microwave emission in high frequency has been frequently observed by NoRH (Kundu et al. 2001; Melnikov et al. 2002; Melnikov et al. 2005; Minoshima et al. 2010; Asai et al. 2013).

The most plausible scenario to interpret the systematic microwave source motions is “asymmetric filament eruptions” (Tripathi et al. 2006; Liu et al. 2009; Liu et al. 2011). In practice, the hard X-ray footpoints motion parallel to NL in the same direction for both footpoints could take place when the filament erupts asymmetrically: One end of the filament rises up by unstable physical condition while the other end anchors to the photosphere and it can lead to a sequential magnetic reconnection in overlying loops aligned with the neutral line (see the illustration of whipping like eruption in Liu et al. 2009). Liu et al. (2011) demonstrated above scenario with the observations of the asymmetric CME eruption and the HXR source motions parallel to the neutral line. Indeed, the microwave source position located in the corona is closer to the acceleration site than HXR source position located on the chromosphere. Thus, the microwave source motion can be a direct indicator of direction of moving acceleration site. On the other hands, recently, Nakariakov & Zimovets (2011) proposed a model that a slow magnetoacoustic wave triggered by an elementary burst may cause another elementary burst in coronal magnetic arcade and it propagates along this arcade. In this model, the elementary burst above or in the loop-top of one edge of the arcade system is enough to produce the motion of high energy emission at the footpoint and near the loop-top.

Note that the high energy emission appears simultaneously in HXR and microwave by injection and precipitation of accelerated particles, and one can expect that their motion should be consistent in the direction and/or its systematic progress. However, in this event, we found that HXR source motion didn’t follow microwave source motion. Furthermore its position was not close to the footpoints where the chromospheric brightening appeared in AIA 304 Å. Such inconsistency can be explained by a presumption as follows: Too strong B field of loops prevents the effective precipitation of trapped electrons by magnetic mirror effect when they are close to footpoints of field (White et al. 2011). At the same time with the above effect, the complex

magnetic field configuration of nonthermal loops, unlike well aligned thermal flare-arcade, may lead to unsystematic motion in hard X-rays. Nonetheless, all the summed results strongly support that our finding of microwave source motion manifests the displacement of the site where accelerated electrons are injected and trapped.

This is the first report of the systematic motion of the microwave source centroid. Even so, it seems to be a common phenomenon which takes place together with the filament/plasma eruption. In fact, hot thermal plasma generated by energy-release process has long cooling time-scale, around several minutes at least, while nonthermal plasma has short lifetime, within 1 seconds for HXR (Kiplinger 1995) and **1~100 seconds for microwaves (Minoshima et al. 2008)**. Thus, nonthermal emission of microwave and hard X-rays is essential to detect and trace the energy-release site than thermal emission of soft X-rays and EUV. The available time cadence of NoRH microwave image is 1 second for steady-mode and 0.1 second for event-mode, while RHESSI HXR needs 4 seconds (Grigis & Benz 2005) and/or 8 seconds (Krucker et al. 2003) average to construct image successfully. In turn, the microwave imaging data from NoRH can effectively trace the time-series of the motion of flare energy-release site even for very short period motion less than 1 second. In this study, the high time cadence data set from NoRH and AIA allowed to examine the source motion and the evolution of the thermal structure in detail during the flare. Thus, the statistical study of them using these data set may provide information on physical conditions crucial for the initiation of the filament/plasma eruption at the position where the microwave source motion starts.

The authors thanks to the referee for helpful comments. This work was carried out by the joint research program of the Solar-Terrestrial Environment Laboratory, Nagoya University. The HMI and AIA data have been used courtesy of NASA/SDO and the AIA, EVE, and HMI science teams. RHESSI is a NASA Small Explorer Mission.

## References

- Asai, A., Kiyohara, J., Takasaki, H., Narukage, N., Yokoyama, T., Masuda, S., Shimojo, M., & Nakajima, H. 2013, *ApJ*, 763, 87
- Bogachev, S. A., & Somov, B. V. 2005, *Astronomy Letters*, 31, 537
- Brueckner, G. E., Howard, R. A., Koomen, M. J., Korendyke, C. M., Michels, D. J., Moses, J. D., Socker, D. G., Dere, K. P., Lamy, P. L., Llebaria, A., Bout, M. V., Schwenn, R., Simnett, G. M., Bedford, D. K., & Eyles, C. J. 1995, *Sol. Phys.*, 162, 357.
- Boerner et al. 2012, *Sol. Phys.*, 275, 41
- Domingo, V., Fleck, B., & Poland, A.I. 1995, *Sol. Phys.*, 162, 1
- Dou, Y., Gary, D. E., Liu, Z., Nita, G. M., Bong, S.-C., Cho, K.-S., Park, Y.-D., & Moon, Y.-J. 2009, *Publication of the Astronomical Society of the Pacific*, 121, 512
- Dulk, George 1985, *ARA&A*, 23, 169
- Forbes, T. G. & Acton, L. W. 1996, *ApJ*, 459, 330



- Guidice, D. A., Cliver, E. W., Barron, W. R., & Kahler, S. 1981, BAAS, 13, 553
- Grigis, P. C. & Benz, A. O. 2005, ApJL, 623, L143
- Hirayama, T. 1974, Sol. Phys., 34, 323
- Huang, G. & Nakajima, H. 2009, ApJ, 696, 136
- Inoue, S., Hayashi, K., Shiota, D., Magara, T., & Choe, G. S. 2013, arXiv:1304.8073
- Jiang, C., & Feng, X. 2013, arXiv:1304.2979
- Kiplinger, A. L. 1995, ApJ, 454, 973
- Krucker, S., Hurford, G. J., & Lin, R. P. 2003, ApJL, 595, L103
- Kundu, M. R., Nindos, A., White, S. M., & Grechnev, V. V. 2001, ApJ, 557, 880
- Lemen et al. 2011, Sol. Phys., 275, 17
- Lin et al. 2002, Sol. Phys., 210, 3
- Liu, R., Alexander, D., & Gilvert, H. R. 2009, ApJ, 691, 1079
- Liu, C., Lee, J., Jing, J., Liu, L., Deng, N., & Wang, H. 2011, ApJL, 721, L193
- Melnikov, V. F., Gorbikov, S. P., Reznikova, V. E., & Shibasaki, K. 2005, Proceeding of the 11th European Solar Physics Meeting, ESA SP-596
- Melnikov, V. F., Shibasaki, K., Reznikova, V. 2002, ApJ, 580, L185
- Minoshima, T., Yokoyama, T., & Mitani, N. 2008, ApJ, 673, 598
- Minoshima, T., Masuda, S., & Miyoshi, Y. 2010, ApJ, 714, 332
- Minoshima, T., Masuda, S., Miyoshi, Y., Kusano, K. 2011, ApJ, 732, 111
- Nakajima, H., Sekiguchi, H., Sawa, M., Kai, K., & Kawashima, S. 1985, PASJ, 37, 163
- Nakajima, H. et al. 1994, Proc. of the IEEE, 82, 701
- Nakariakov, V. M. & Zimovets, I. V. 2011, ApJL, 730, L27
- Reznikova, V. E., Melnikov, V. F., Ji, H., & Shibasaki, K. 2010, ApJ, 724, 171
- Scherrer, P. H., Schou, J., Bush, R. I., Kosovichev, A. G., Bogart, R. S., & Hoeksema, J. T. 2012, Sol. Phys., 275, 207
- Shibata, K., Masuda, S., Shimojo, M., Hara, H., Yokoyama, T., Tsuneta, S., Kosugi, T., & Ogawara, Y. 1995, ApJL, 451, L83
- Somov, B. V., & Kosugi, T. 1997, ApJ, 485, 859
- Tripathi, D., Isobe, H., Mason, H. E. 2006, *Å*, 453, 1111
- Yokoyama, T., Nakajima, H., Shibasaki, K., Melnikov, V. F., & Stepanov, A. V. 2002, ApJ, 576, L87
- White, S. M., Thomas, R. J. & Schwartz, R. A. 2005, Sol. Phys., 227, 231
- White, S. M., Benz, A. O., Christe, S., Farnik, F., Kundu, M. R., Mann, G., Ning, Z., Raulin, J.-P., Silva-Valio, A. V. R., Saint-Hilaire, P., Vilmer, N., Warmuth, A. 2011, Space Sci. Rev., 159, 225

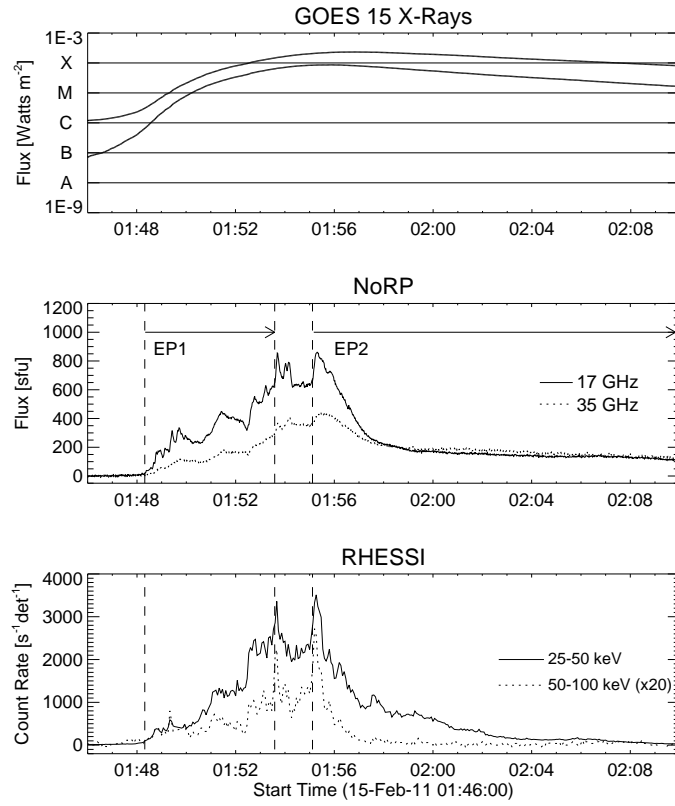


**Fig. 1.** Time profiles of fluxes from GOES X-rays (top), NoRP 17 and 35 GHz (middle), and RHESSI 25-50 and 50-100 keV (bottom). Vertical dashed lines are start and end times of two episodes (EP1 and EP2) of microwave source motion

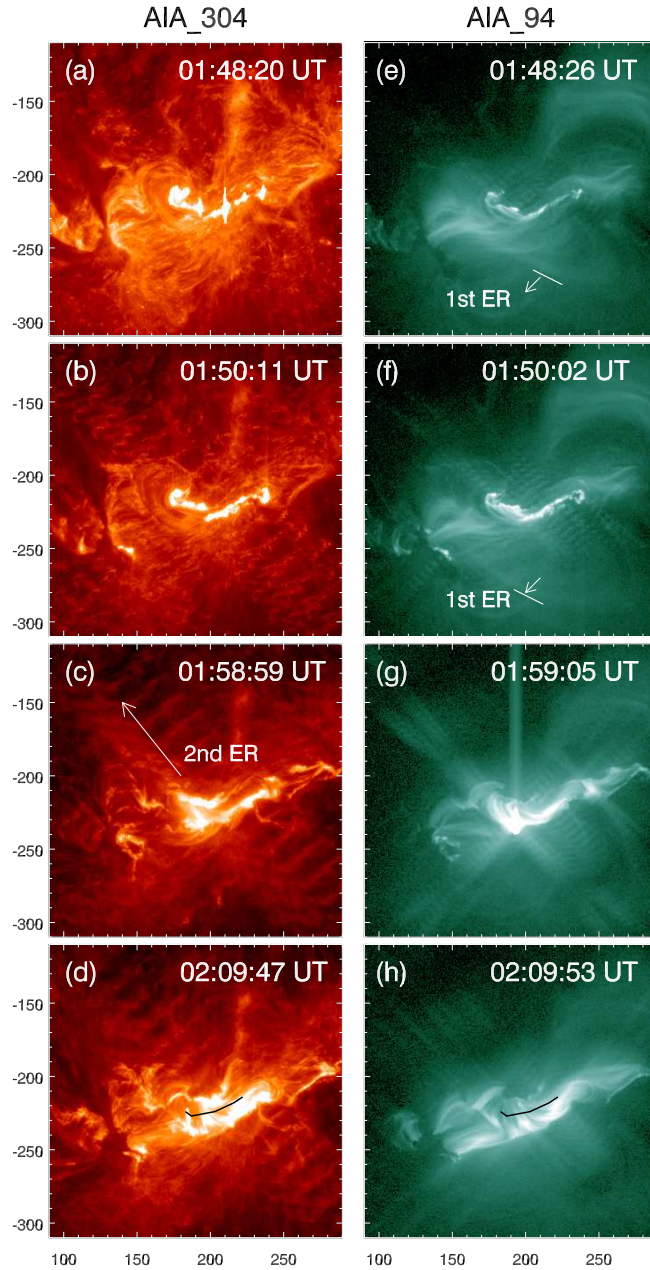


**Fig. 2.** Sequential images from the AIA two channels, 304 Å (left column) and 94 Å (right column). The 94 Å channel exhibits the manifestation of the first eruption (1st ER) in (e) and (f): The edge of a bundle of coronal loops, which is marked by solid lines, expands along a white arrow. The 304 Å channel exhibits the second eruption (2nd ER) in (c): bulk of plasma erupts along a white arrow. The neutral line determined by the HMI magnetogram (Figure 4) is superimposed on the bottom panels as a black line

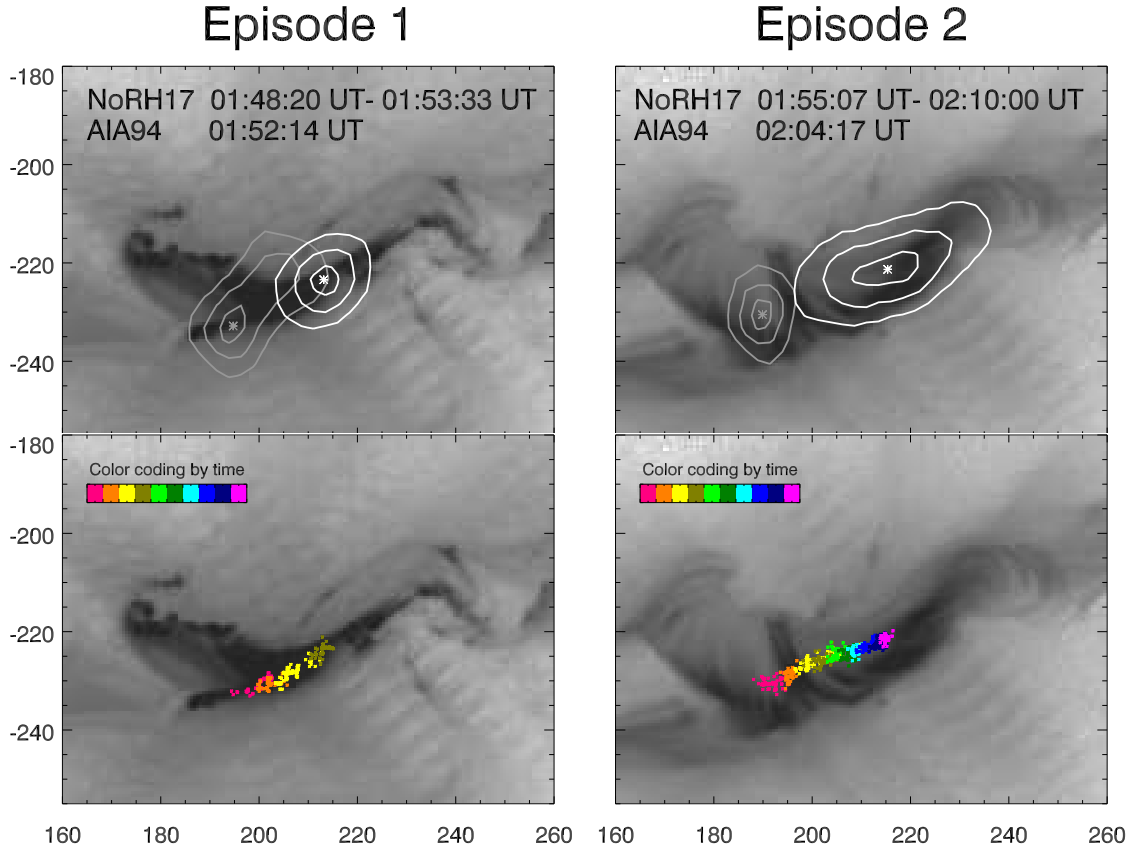


**Fig. 3.** *Top panels:* NoRH 17 GHz contours on AIA 94 Å image for two episodes of the microwave source motion, episode1 (left) and episode2 (right). The levels of contour are 70, 90, and 95 % of the maximum  $T_B$ . Gray and white contours were obtained at the start and the end time of the source motion, respectively. *Bottom panels:* Overall positions of microwave source centroid during episode1 (left) and episode2 (right). Colors of each symbol are coded by time. Each color contains 90 seconds and the colorbar covers 15 minutes with 10 colors.

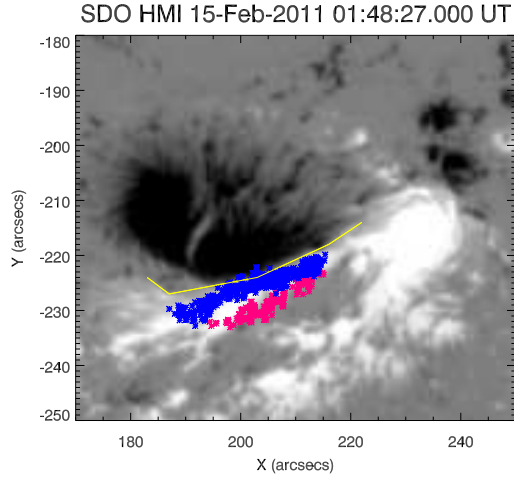


**Fig. 4.** Microwave source centroids for EP1 (red) and EP2 (blue) superposed on the HMI magnetogram. The neutral line is denoted by a yellow line.

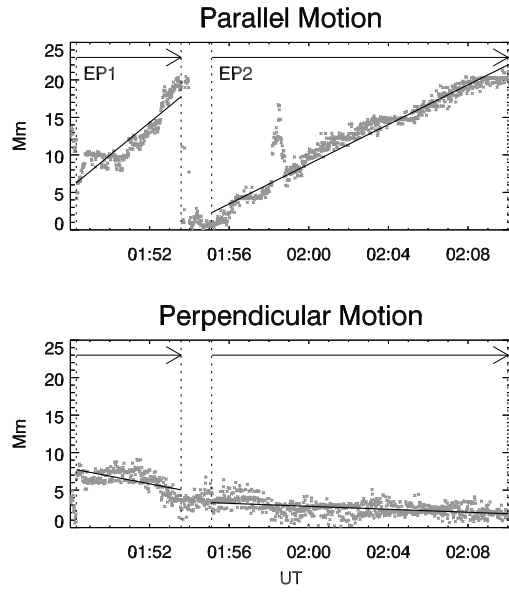


**Fig. 5.** Time evolution of the source positions parallel to the NL (top) and perpendicular to the NL (bottom). The velocity of motions was derived by linear fit of the scattered plots of positions (solid lines).

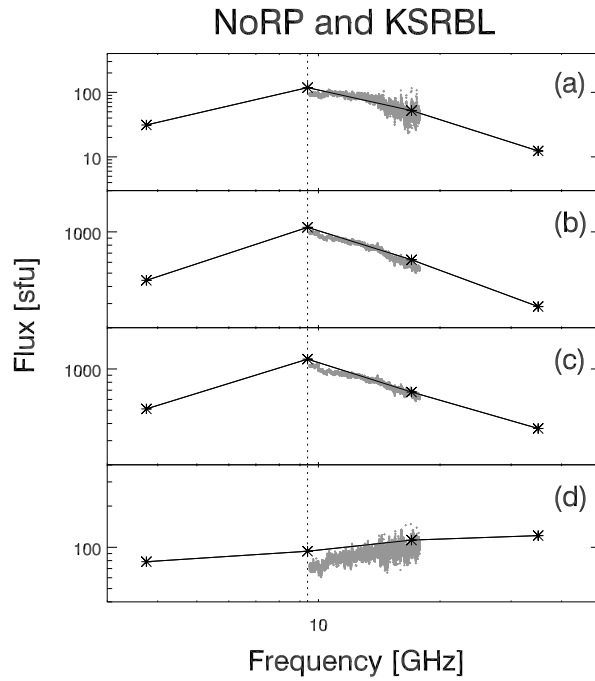


**Fig. 6.** Microwave spectra obtained by NoRP four channels of 3.75, 9.4, 17, and 35 GHz (asterisks) and by KSRBL continuous spectra in the range of 9.5–18 GHz with 1 MHz resolution (scatter plot with gray color) during the flare. (a) and (b) were obtained at 01:48:34 UT and at 01:53:34 UT during episode 1. (c) and (d) were obtained at 01:55:09 UT and at 02:09:59 during episode 2. Vertical dashed line marks 9.4 GHz of NoRP which roughly indicates the turnover frequency.